



Synthesis of Chitosan –g-Acrylamide-Co-Acrylic Acid /Ag Nanocomposite For Extended Wound Healing Application

Yousaf Dawood ^a, Hameed M. Alkubaisi ^b, Oqba N. Al-Shayea ^{a*}, A. S. Montaser ^{c*}



^{a*} College of Pharmacy, University of Anbar, Ramadi, Anbar, Iraq

^b Applied Chemistry Department, College of Applied Science, Fallujah University, Fallujah, Iraq

^{c*} Pre-treatment and Finishing of Cellulose Based Textiles Department, National Research Centre, Dokki, Giza

Abstract

New nanocomposite based on chitosan and acrylamide and silver nanoparticles has been prepared to produce wound dressing has superior properties as Hemostatic and antibacterial activity. Chitosan successfully grafted with acrylamide via free radical copolymerization using potassium persulphate. Four different chitosan grafted acrylamide prepared and fully characterized through nitrogen content and ATR/IR. Cs-g- PAAM partially hydrolyzed at basic condition in presence of silver nitrate in order to prepare Cs-g-PAAM-co-PAAC/Ag nanocomposite. The optimum condition for preparing homogenous and well distributed was examined using grafted polymers were characterized using TEM and UV-vis absorption. Cs:PAAM (1:1) pH 11 and 120 min showed homogenous spherical silver nanoparticles and distributed particles lying at nanosize range between 10-30 nm. SEM-EDX and XRD used to confirm binding silver to chitosan hybrid chains forming newly nanocomposite. Produced composite showed complete solubility at neutral medium condition that qualifies produced composite to be used at different medical and industrial applications.

Keywords: Chitosan, PAAM, AgNPs

1. Introduction

Most of death cases on the battlefield usually correlated with severe bleedings[1]. It is expected that decreasing this number can be exhibited by enhancing hemorrhage methods and devices[2]. Not only enhancing hemorrhage control would improve military but also nonmilitary settings, e.g., in hospitals or veterinary clinics as well[3]. Incorporation of Hemostatic components and wound dressings may be made by a variety of methods[4]. These methods include coating of the substrate with one or more of the hemostatic compositions and a polymeric binder prepared from biocompatible material(s), water-soluble material(s), water-swallowable material(s), bio-resorbable material(s) and/or other material(s) containing embedded and/or co-deposited active and/or functional water soluble

particles[5]. Chitosan as a second abundant natural polymer on the earth, it is unique formula which contains hydroxyl and amino function, utilized for many medical applications as antibacterial and biodegradable polymer[6-8]. Unfortunately, chitosan solubility at acidic medium stands a barrier for many applications. Modifying chitosan through etherification and grafting was published [9, 10]. Furthermore, in order to increase chitosan hemostatic properties it's grafted with superabsorbent monomer as acrylamide and acrylic acid or acrylamide-co-acrylic acid[11, 12]. Chitosan grafted to acrylic acid and acrylic derivatives through free radical copolymerization utilizing many redox systems as potassium persulphate, ammonium persulphate, cerium citrate....etc[13]. Incorporation nanoparticles with hydrogels based on chitosan was recently

*Corresponding author e-mail: [A.S.Montser](mailto:A.S.Montser;); (abohabbiba2012@gmail.com)

and ON Al-Shayea a(ds.dr.oqbanafia@uoanbar.edu.iq)

Receive Date: 23 December 2020, Revise Date: 16 February 2021, Accept Date: 10 May 2021

DOI: 10.21608/EJCHEM.2021.53441.3127

©2021 National Information and Documentation Center (NIDOC)

published. Chitosan derivatives not only used as anti-Hemostatic agent, but also work as reducing and stabilizing for silver nanoparticles as well. Chitosan grafted to acrylamide through free radical copolymerization forming chitosan -g- acrylamide. Cs-g-PAM crosslinked forming hydrogel [14, 15]. Herein, Cs-g-PAAm produced through radical polymerization with different ratio, produced polymers hydrolyzed forming Cs-g-PAM-co-PA/AgNPs nanocomposite. Produced composites characterized with modern tools as ATR/IR, UV-vis spectrophotometer and TEM. The produced graft copolymer successfully used for reducing silver salts forming nanocomposite hoped to be applied on cotton fabrics to be used as wound dressing characterized with hemostatic and antibacterial properties.

2. Materials and methods

2.1. Materials

Chitosan high molecular weight 600kx purchased from sigma-aldrich company, while acrylamide was bought from Flukabanch in Egypt. Silver nitrate purchased from sisco, India. All other chemicals are laboratory grades.

2.2. Methods

2.2.1. Preparation of chitosan-g- PAAm-co-PAAc/Ag nanocomposite

Chitosan grafted on poly acrylamide as reported elsewhere. Chitosan solution solubilized at 1% acetic acid and heated until reach 60°C. potassium persulfate with definite amount added to reaction medium followed by different amount of acrylamide powder to produce four different chitosan grafted solution namely Cs-g-PAAm1, Cs-g-PAAm2, Cs-g-PAAm3 and Cs-g-PAAm4. Produced chitosan derivatives characterized using ATR/IR process and nitrogen content used to confirm grafting process via exploring newly functions and changing at chemical formula. The four chitosan derived exposed to alkaline hydrolysis using 0.1N NaOH in presence of 0.1N AgNO₃ to produce Cs-g-PAAm-co-PAAc/Ag nanocomposite.

Produced nanocomposite ultrasonicated examined under UV-vis spectrophotometer, TEM, SEM-EDX and XRD techniques used to visualize formation, homogeneity and dispersity [9, 16, 17].

3. Results and Discussion

Producing chitosan derivatives through radical copolymerization widely reported, chitosan reacted through radical formation of oxy acids and persulphates [18]. Produced chitosan derivatives

usually characterized with newly function differ from chitosan as negativity, conductivity and solubility. Fig.1 describes the chemical modification of chitosan through grafting using potassium persulphate as initiator for grafting process. The grafted chitosan polymer exposed to alkaline treatment in presence of silver salt to produce Cs-g-PAAm-co-PAAc/Ag nanocomposite

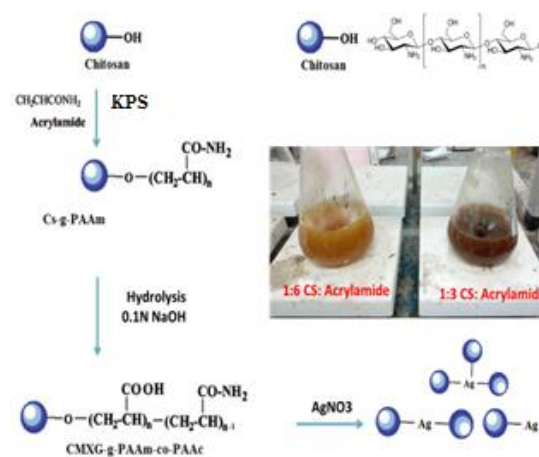


Fig. 1: scheme of producing Cs-g-PAAm-co-PAAc/Ag nanocomposite

3.1. ATR/IR

Fig. 2 shows the ATR/IR of chitosan, acrylamide, chitosan-g-PAAm-co-PAAc and chitosan-g-PAAm-co-PAAc/Ag nanocomposite. The characteristic peaks of glucose units of chitosan are as follows. Chitosan spectrum exhibited the distinctive absorption bands at 1658 cm⁻¹ (Amide I), 1595 cm⁻¹ (-NH₂ bending) and 1314 cm⁻¹ (Amide III). The absorption bands at 1154 cm⁻¹ (anti-symmetric stretching of the C-O-C bridge), 1082 and 1032 cm⁻¹ (skeletal vibrations involving the C-O stretching) are characteristic of its saccharide structure [19]. While as, acrylamide showed 1563 cm⁻¹ related to carboxylic group and its increases with hydrolyses to reach 1670 cm⁻¹. To characteristic peaks The spectrum of Cs-g-PAAm-co-PAAc two significant peaks at 1650 cm⁻¹ and 1444 cm⁻¹ which represents amide group of acrylamide and symmetric stretching of -COO- ions of acrylic acid.

Comparing chitosan grafted polymer and chitosan grafted nanocomposite, more sharpness for 600 cm⁻¹ peak that belongs to presence of AgNPs.

Grafting process of chitosan and acrylamide with different ratios (1:1, 1:3, 1:5, 1:7) presented at Fig. 3. named Cs-g-PAM1, Cs-g-PAM2, Cs-g-PAM3 and Cs-g-PAM4 respectively. The figure showed decrement at hydroxyl group intensity, resulted from hydroxyl group grafting with acrylamide monomer. Besides, the increment of amide bond increases with

increasing acrylamide monomer ratio to chitosan. Logically, this increment is directly proportional with acrylamide monomer percent's. this increment results from more blocking to hydroxyl groups of chitosan

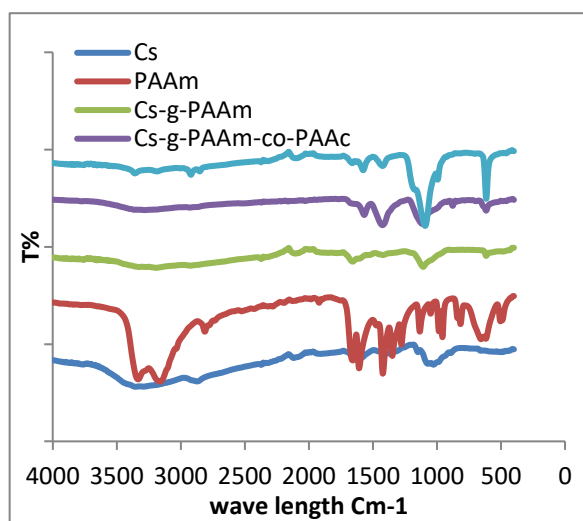


Fig. 2. ATR/IR of chitosan, PAAm, Cs-g-PAAm, Cs-g-PAAm-co-PAAc and Cs-g-PAAm-co-PAAc/Ag nanocomposite

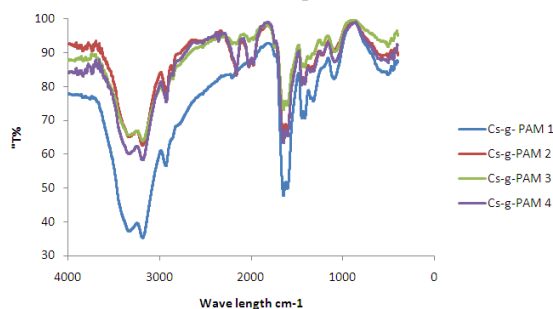


Fig. 3. ATR/IR of Chitosan grafted acrylamide with ratios (1:1, 1:3, 1:5, 1:7) named Cs-g-PAM1, Cs-g-PAM2, Cs-g-PAM3 and Cs-g-PAM4

3.2. Grafting Efficiency and Nitrogen content

The growing interest of environment and nature as using low toxic compounds and easy handle chemical instead of hazard one are growing last decade. Synthesis of silver nanoparticles from either acrylic or acrylic derivative is published elsewhere. Herein, chitosan as biopolymer grafted with acrylamide used to produce silver nanoparticles. Needless to mention that chitosan as a biopolymer will reduce the toxicity compared to acrylamide. On the other side, acrylamide used to improve chitosan solubility and acquiring hemostasis property to chitosan. Furthermore, create g new function assist silver cation reduction. In addition, Easy handling of acrylamide compared to acrylic acid, and easy conversion of polyacrylamide at basic medium to acrylic acid candidate acrylamide to be used as precursor for acrylic acid synthesis. The dual action

of basic condition at acrylamide conversion and ambient medium for preparing silver nanoparticles inspire our group to examine silver nanoparticles formation at chitosan grafted acrylamide at different saponification of chitosan –g-acrylamide –co-acrylic acid.

Grafting process of chitosan and acrylonitrile are clearly appeared at N% analysis, it's clearly appeared at table 1 increasing nitrogen percent with grafting process ratios. It's increased from 7% to chitosan 25, 26.54, 30.17, 33.69 and 39.89 for chitosan grafted acrylonitrile 1:1, 1:3, 1:5 and 1:7. The results confirm more grafting of acrylamide on to chitosan chain with increasing acrylamide monomer ratio to chitosan[20].

3.3. UV and histogram

Fig.4 of UV – vis spectra of synthesized silver nanoparticles using 1% Cs-g-PAM (1:1) at different time intervals. It's stated that absorption peak of produced silver nanoparticles located between 400-500 nm depends on size and shapes. It's clearly appeared that with increasing time from 15 min to 60 min the intensity of absorption peak increases. It may be attributed to more chance gives to chitosan grafted chains for reducing and stabilizing produced AgNPs[21].

Fig.5 illustrates the effect of pH medium on the silver nanoparticle formation. It's clear that absorption peak of silver nanoparticles increases with increasing pH values. The peak intensity increases sharply at basic medium. It may attributed to conversion of amide group into carboxylic group which may be more powerful at reducing or turning silver into silver nanoparticles [22].

The effect of grafting ratio of chitosan and chitosan acrylamide showed at fig. 6. it's clear that intensity peak of synthesized AgNPs decrease with increasing monomer ration to chitosan. It may be attributed to acrylamide self - polymerization that affects negatively on reducing power. Interestingly, the aforementioned results may be useful at reducing toxicity of grafted chitosan[23].

Table 1: Grafting efficiency and nitrogen percent of Cs-g-PAAm.

Cs(Wt.)	Acrylamide(Wt.)	W2	G%	N%
1	0	0	0	7
1	1	1.652	84	25
1	3	1.8642	86.42	26.54
1	5	3.090	209	30.17
1	7	3.7042	270	33.69

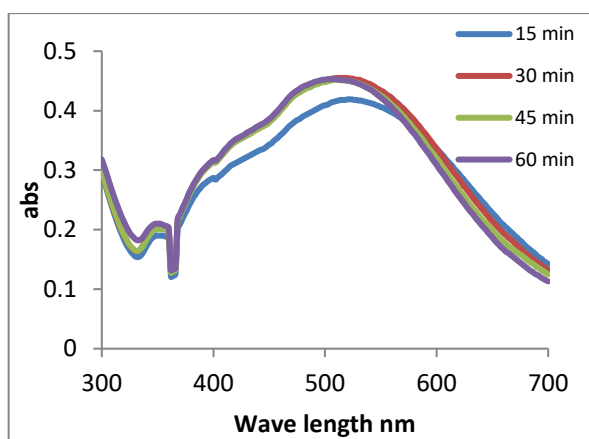


Fig. 4: UV-vis spectrum of Cs-g-PAAm-co-PAAc/Ag nanocomposite at different duration.

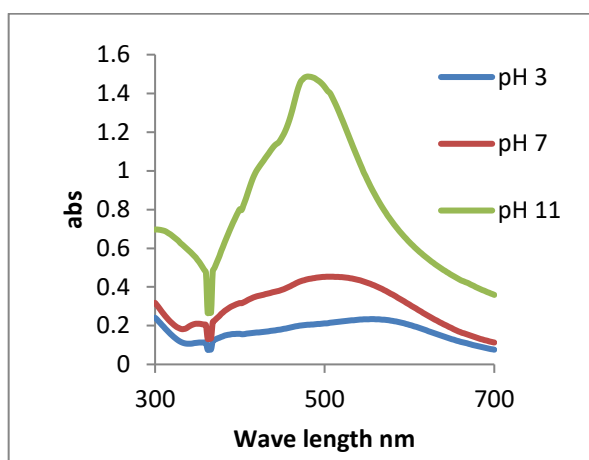


Fig. 5: UV-vis spectrum of Cs-g-PAAm-co-PAAc/Ag nanocomposite at different pHs.

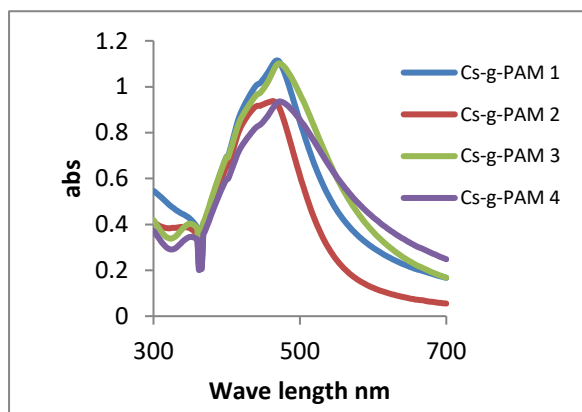


Fig. 6: UV-vis spectrum of Cs-g-PAAm-co-PAAc/Ag nanocomposite at different grafting ratios.

3.4. Transmission Electron Microscope (TEM)

It is obvious from TEM images and histograms (Fig. 7) that Cs-g-PAM-co-Ac/AgNPs nanocomposite with a size range of 120-200 nm is successfully prepared using chemical reduction method utilizing Cs-g-PAM-co-AC as reducing and stabilizing agent at neutral medium but it's

characterized with inhomogeneity and large size. Fig 7b, c, d, and e shows that the silver nanoparticles prepared at basic medium are characterized by homogeneity and dispersity within size range 30-40 nm. Grafted chitosan solution appears at the pictures background adhesive to the prepared nanometals. It is further observed that the decrement in histogram size distribution of the samples is due to the existence of AgNPs.[24-27]

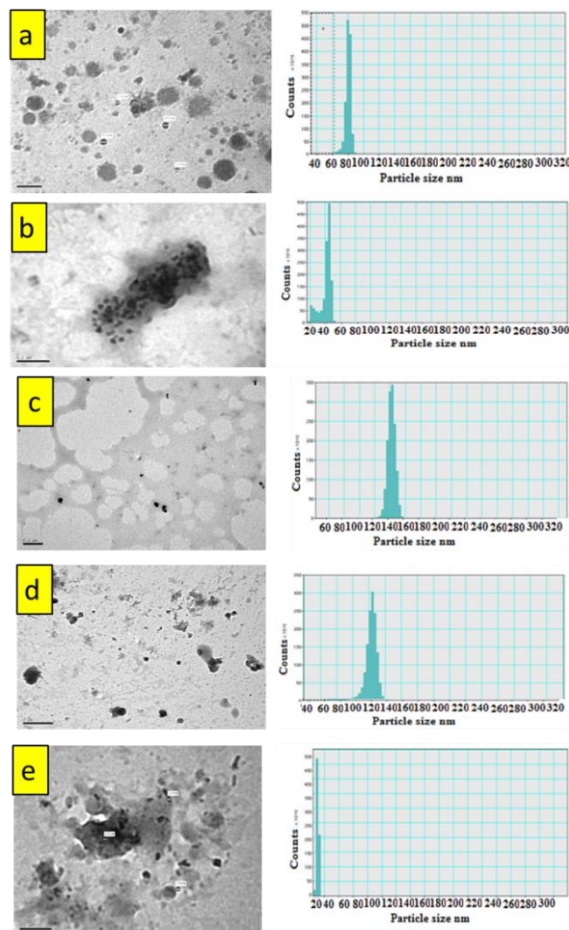


Fig. 7: TEM-EDX images of CS-g-PAAm-co-PAAc/Ag nanocomposites ratio (1:1) at pH7 and (b-e)CS-g-PAAm-co-PAAc/Ag nanocomposites pH 11 with different ratios (1:1), (1:3), (1:5) and (1:7) respectively.

The low percent of acrylamide grafted on to chitosan showed high reducing power compared with high percent. As shown in digital images Fig .8. More dark brown color belongs to chitosan grafted with low monomer concentration of acrylamide. This may be interpreted as follow: a) by increasing acrylamide monomer formed more homopolymer formed which prefer silver complexation than reduction. b) low monomer reactant percent of acrylamide assist fully converting amide group to carboxyl group compared with high amount of acrylamide[28].

From this point of view low concentration of Cs-g-PAAM-co-PAAc/Ag nanocomposite candidates to be applied on cotton fabrics to be used as hemostatic and antibacterial wound dressing.

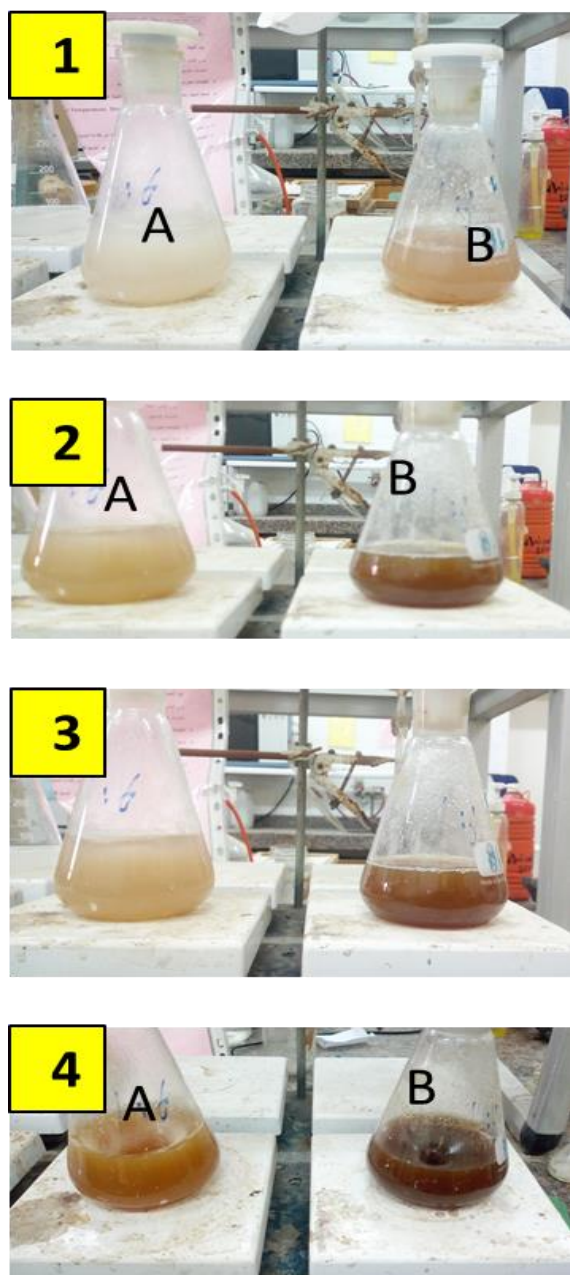


Fig. 8: Digital imaging for reduction of silver nanoparticles using a) low (1:3) and b) high (1:6) Cs-g-PAAM-co-PAAc Where: 1) at 30 min, b) 60 min, 3) 90 min and 4) 120 min

3.5. Scanning Electron Microscope- Electron Dispersed X-ray (SEM-EDX)

SEM illustrates the microstructure of chitosan and chitosan-g-PAAM-co-PAAc/Ag nanocomposite in order to figure out the effect of grafting process and nanocomposite formation. Chitosan microstructure shows roughness layers with coagulated particles at high resolution. On the other hand, chitosan

nanocomposites showed a sponge like structure and numerous circular spherical particles with approximately uniform size (2 to 5mm). These observations are in good agreement with expectation about forming silver centered coagulating chitosan derivatives chains. EDX of chitosan showed clearly its elemental constituents as C, O and N. while as Ag element appeared clearly at EDX of chitosan-g-PAAM-co-PAAc/Ag nanocomposite beside chitosan besides K, S which resulted from radical polymerization used $K_2S_2O_7$.

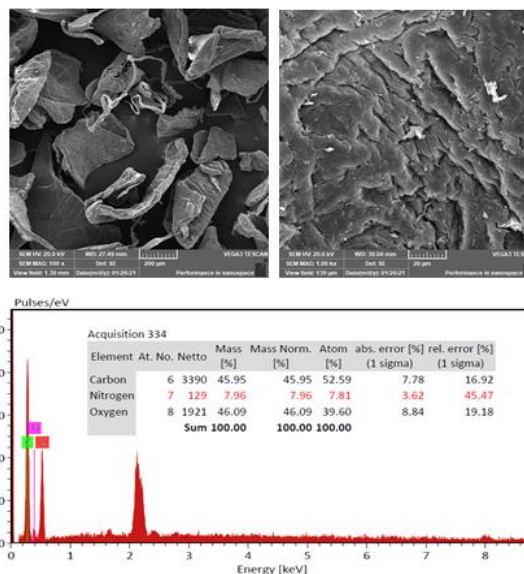


Fig. 9: SEM-EDX of chitosan and Chitosan-g-PAAM-co-PAAc/Ag nanocomposite

3.6. X-ray Diffraction (XRD)

The structural properties of the synthesized CS and Cs-g-PAM-co-PAAc/Ag nanocomposite were analyzed using the XRD technique. The obtained XRD pattern for chitosan is shown in Fig. 10. The broadened peaks appeared at 2 θ values of 11.7 and 20.2° are belongs to amorphous nature of the polymer. Anew peaks are appearing are results of grafting and hydrolyzing process. The XRD pattern of silver nanocomposite clearly indicates the formation of silver peaks which obtained at 2 θ values of 37.9, 44.0 and 63.9° which in agreement with our previous literatures [29].

3.7. Chitosan- g-PAAM-co-PAAc/Ag nanocomposite solubility

Produced composite dried and solubilized at neutral medium (pH 7) to examine its applicability. Chitosan-g-PAAM-co-PAAc/Ag nanocomposite showed complete water solubility as shown in Fig. 10. The solubility of modified chitosan with acrylamide and its hydrolyzed nanocomposite attributed to new carboxylic group that responsible of

solubility in wide pH range [24-26]. Produced composites expected to be used for industrial and medical applications lonely or incorporated with synthesized antibacterial materials[27].

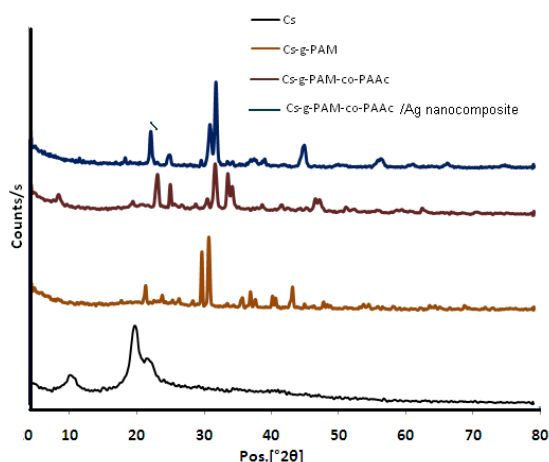


Fig.10. X-Ray Diffraction of Chitosan and its composite

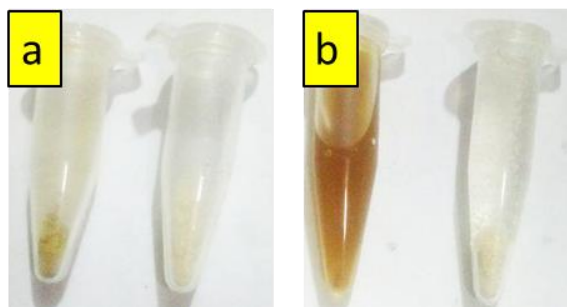


Fig. 10: Digital images for Chitosan and Cs-g-PAAm-co-PAAc/Ag nanocomposite a)Solid state and b) solubilized state.

4. Conclusion

Chitosan-g-PAAm-co-PAAc/Ag nanocomposite successfully prepared through alkaline hydrolyses of Cs-g-PAAm in presence of silver salt. Under TEM exploration, produced composite showed homogeneity at low monomer concentration grafted to chitosan. Produced composite expected to be used for treating cotton fabrics to produce cotton wound dressing characterized by hemostatic and antibacterial activity.

5. References

[1] U. Katzenell, N. Ash, A. Tapia, G. Abebe Campino, E. Glassberg, Analysis of the Causes of Death of Casualties in Field Military Setting, *Military medicine* 177 (2012) 1065-8.

[2] R. Sahni, J. Weinberger, Management of intracerebral hemorrhage, *Vasc Health Risk Manag* 3(5) (2007) 701-709.

[3] H.T. Peng, Hemostatic agents for prehospital hemorrhage control: a narrative review, *Military Medical Research* 7(1) (2020) 13.

[4] J.V. Edwards, E. Graves, N. Prevost, B. Condon, D. Yager, J. Dacorta, A. Bopp, Development of a Nonwoven Hemostatic Dressing Based on Unbleached Cotton: A De Novo Design Approach, *Pharmaceutics* 12(7) (2020).

[5] M. Kabiri, S. Hojjati Emami, M. Rafienia, M. Tahriri, Preparation and characterization of absorbable hemostat crosslinked gelatin sponges for surgical applications, *Current Applied Physics* 11 (2011) 457-461.

[6] A.S. Montaser, A.R. Wassel, O.N. Al-Shaye'a, Synthesis, characterization and antimicrobial activity of Schiff bases from chitosan and salicylaldehyde/TiO₂ nanocomposite membrane, *International Journal of Biological Macromolecules* 124 (2019) 802-809.

[7] A.S. Montaser, F.A. Mahmoud, Preparation of Chitosan-grafted-Polyvinyl acetate Metal Nanocomposite for producing Multifunctional Textile Cotton Fabrics, *International Journal of Biological Macromolecules* 124 (2019) 659-666.

[8] A.A. Hebeish, M.A. Ramadan, A.S. Montaser, A.M. Farag, Preparation, characterization and antibacterial activity of chitosan-g-poly acrylonitrile/silver nanocomposite, *International Journal of Biological Macromolecules* 68 (2014) 178-184.

[9] A. Hebeish, A.S. Aly, M.A. Ramadan, M.M.A. El-Hady, A.S. Montaser, A.M. Farag, Establishment of optimum conditions for preparation of silver nanoparticles using carboxymethyl chitosan, *Egyptian Journal of Chemistry* 56(3) (2013).

[10] A. Abdel-Mohsen, A. Aly, R. Hrdina, A. Montaser, A. Hebeish, Biomedical textiles through multifunctionalization of cotton fabrics using innovative methoxypolyethylene glycol-N-chitosan graft copolymer, *Journal of Polymers and the Environment* 20(1) (2012) 104-116.

[11] H. Ferfera-Harrar, N. Aiouaz, N. Dairi, A.S. Hadj-Hamou, Preparation of chitosan-g-poly(acrylamide)/montmorillonite superabsorbent polymer composites: Studies on swelling, thermal, and antibacterial properties, *Journal of Applied Polymer Science* 131(1) (2014).

[12] N.S. Elshemy, A.G. Hassabo, Z.M. Mahmoud, K. Haggag, Novel Synthesis of Nano-emulsion Butyl Methacrylate/Acrylic Acid via Micro-emulsion Polymerization and Ultrasonic Waves, *Journal of Textile and Apparel, Technology and Management* 10(1) (2016) 1-16.

[13] A. Shanmugapriya, A. Srividhya, R. R, S. P.N, Graft copolymerization of chitosan with acrylic acid used in waste water treatment, *Int J Environ Sci* 1 (2011) 2086-2095.

[14] Z. Ali, J. Venkatesan, S. Kim, S. P.N, Beneficial Effect of chitosan-g- Polyacrylamide Copolymer in Removal of Heavy Metals from Industrial Dye Effluents, *International Journal of Environmental Sciences* 1 (2011).

[15] A.G. Hassabo, A.L. Mohamed, Multiamine Modified Chitosan for Removal Metal Ions from their Aqueous Solution *BioTechnology: An Indian Journal* 12(2) (2016) 59-69.

[16] A.S. Montaser, M.A. Ramadan, A.A. Hebeish, Facile way for synthesis silver nanoparticles for obtaining antibacterial textile fabrics, *Journal of Applied Pharmaceutical Science* 6(06) (2016) 139-144.

- [17] A.S. Montaser, Physical, mechanical and antimicrobial evaluations of physically crosslinked PVA/chitosan hydrogels containing nanoparticles, *Journal of Applied Pharmaceutical Science* 6(05) (2016) 001-006.
- [18] K.V.H. Prashanth, R.N. Tharanathan, Studies on graft copolymerization of chitosan with synthetic monomers, *Carbohydrate Polymers* 54(3) (2003) 343-351.
- [19] A.J.M. Al-Karawi, Z.H.J. Al-Qaisi, H.I. Abdullah, A.M.A. Al-Mokaram, D.T.A. Al-Heetimi, Synthesis, characterization of acrylamide grafted chitosan and its use in removal of copper(II) ions from water, *Carbohydrate Polymers* 83(2) (2011) 495-500.
- [20] S.I. Siafu, Silicone Doped Chitosan-Acrylamide Coencapsulated Urea Fertilizer: An Approach to Controlled Release Fertilizers, *Journal of Nanotechnology* 2017 (2017) 8490730.
- [21] M. Darroudi, M. Ahmad, R. Zamiri, A. Khorsand Zak, A. Abdullah, N. Ibrahim, Time-dependent effect in green synthesis of silver nanoparticles, *International Journal of Nanomedicine* 6 (2011).
- [22] P. Traiwatcharanon, K. Timsorn, C. Wongchoosuk, Effect of pH on the Green Synthesis of Silver Nanoparticles through Reduction with Pistiastratiotes L. Extract, *Advanced Materials Research* 1131 (2015) 223-226.
- [23] M. Venkatesham, D. Ayodhya, A. Madhusudhan, N. Veera Babu, G. Veerabhadram, A novel green one-step synthesis of silver nanoparticles using chitosan: catalytic activity and antimicrobial studies, *Applied Nanoscience* 4(1) (2014) 113-119.
- [24] A.V. Vivek, P. Maiti, R. Dhamodharan, Synthesis of Silver Nanoparticles Using a Novel Graft Copolymer and Enhanced Particle Stability via a "Polymer Brush Effect", *Macromolecular Rapid Communications* 29 (2008) 737.
- [25] A.G. Hassabo, S. Shaarawy, A.L. Mohamed, A. Hebiesh, Multifarious cellulosic through innovation of highly sustainable composites based on Moringa and other natural precursors, *Int. J. Biol. Macromol.* 165 (2020) 141-155.
- [26] A.L. Mohamed, A.G. Hassabo, Cellulosic fabric treated with hyperbranched polyethyleneimine derivatives for improving antibacterial, dyeing, pH and thermo-responsive performance, *Int. J. Biol. Macromol.* 170 (2021) 479-489.
- [27] M. Zayed, H. Ghazal, H. Othman, A.G. Hassabo, Psidium Guajava Leave Extract for Improving Ultraviolet Protection and Antibacterial Properties of Cellulosic Fabrics, *Biointerf. Res. Appl. Chem.* 12(3) (2022) 3811 - 3835.
- [28] Z. Gün Gök, A. Demiral, O. Bozkaya, M. Yiğitoğlu, In situ synthesis of silver nanoparticles on modified poly(ethylene terephthalate) fibers by grafting for obtaining versatile antimicrobial materials, *Polymer Bulletin* (2020).
- [29] A.L. Mohamed, M.E. El-Naggar, T.I. Shaheen, A.G. Hassabo, Novel nano polymeric system containing biosynthesized core shell silver/silica nanoparticles for functionalization of cellulosic based material, *Microsys. Technol.* 22(5) (2016) 979-992.